




Ultrafast thin-disk multipass amplifier with 720 mJ operating at kilohertz repetition rate for applications in atmospheric research

CLEMENS HERKOMMER,^{1,2,*}  PETER KRÖTZ,¹ ROBERT JUNG,¹ SANDRO KLINGEBIEL,¹ CHRISTOPH WANDT,¹ ROBERT BESSING,¹ PIERRE WALCH,³ THOMAS PRODUIT,⁴  KNUT MICHEL,⁵ DOMINIK BAUER,⁶ REINHARD KIENBERGER,² AND THOMAS METZGER¹

¹TRUMPF Scientific Lasers GmbH & Co. KG, Feringastr. 10a, 85774 Unterföhring, Germany

²Technische Universität München, Physik-Department E11, James-Franck-Str. 1, 85748 Garching, Germany

³LOA, ENSTA ParisTech, CNRS, Ecole polytechnique, 828 Bd des Maréchaux, 91762 Palaiseau, France

⁴Groupe de Physique Appliquée, Université de Genève, Ch. de Pinchat 22, 1211 Genève 4, Switzerland

⁵TRUMPF Laser- und Systemtechnik, Johann-Maus-Str. 2, 71254 Ditzingen, Germany

⁶TRUMPF Laser GmbH, Aichhalder Str. 39, 78713 Schramberg, Germany

*Clemens.Herkommer@TRUMPF.com

Abstract: We present an ultrafast thin-disk based multipass amplifier operating at a wavelength of 1030 nm, designed for atmospheric research in the framework of the Laser Lightning Rod project. The CPA system delivers a pulse energy of 720 mJ and a pulse duration of 920 fs at a repetition rate of 1 kHz. The 240 mJ seed pulses generated by a regenerative amplifier are amplified to the final energy in a multipass amplifier via four industrial thin-disk laser heads. The beam quality factor remains ~ 2.1 at the output. First results on horizontal long-range filament generation are presented.

© 2020 Optical Society of America under the terms of the [OSA Open Access Publishing Agreement](#)

1. Introduction

During the past two decades, atmospheric research has been propelled by studies on laser filamentation, enabled by high energy ultrafast laser technology. The advent of CPA-based Ti:Sa laser technology allowed to investigate the dynamics of the self-channeling process [1] prompted by terawatt peak powers within femtosecond pulse durations. The ability to remotely deliver high intensities by laser filaments has unlocked new potential in atmospheric applications such as laser-induced water condensation [2–4], remote pollution monitoring [5–7], free-space optical communication through fog [8–10], and the laser-based lightning rod [11–15]. For the latter, the increased electrical conductivity associated with the path of the laser pulses during filamentation can trigger and guide high-voltage (HV) electric discharges (i.e., the lightning). Thus the natural sparking which typically occurs along an erratic path can be controlled and overridden [11,16].

The Laser Lightning Rod (LLR) project [17–19] addresses lightning protection with a specifically designed laser source. The completion of the permanent conductive channel from ground to clouds requires ultrashort pulses with terawatt peak powers at kHz repetition rates. Although the lifetime of the free carriers in the plasma generated by the laser filaments is only short-lived on the order of $< 1 \mu\text{s}$, a channel of heated and under-dense air with reduced resistivity can be initiated and sustained over several milliseconds by the large lineic energy deposited in the filaments [19–21]. It was shown that there is a cumulative effect when increasing the repetition rate towards the inverse channel lifetime, sustaining a permanent conductive channel, that can significantly reduce the breakdown voltage in air [10,22].

The laser source for the LLR project must therefore operate at a kilohertz repetition rate and provide ultrashort pulses with sufficient pulse energy to reach terawatt-class peak powers. Ti:Sa-based lasers can today provide hundreds of mJ of pulse energy at pulse durations below 100 fs (e.g., ENSTA TT Mobile, Amplitude technologies). However, their average powers are currently limited to a few tens of watts. In contrast, kilowatt average power levels are routinely achieved with Yb-based diode-pumped ultrafast laser systems. Their architecture can be based on slab [23,24], fiber [25,26] or thin-disk geometries [27]. Pulse energy scaling has been particularly successful in thin-disk based regenerative amplifiers. Recently, pulse energies above 200 mJ [28,29] with multi-kilowatt average powers [30] and pulse durations as short as <500 fs [31,32] have been demonstrated. These achievements bring the possibility of laser driven lightning protection, as in the LLR project, closer than ever. In addition, such laser systems deliver near-diffraction-limited beam quality, unravelling new insights in high-intensity physics and dazzling new applications. The generation of secondary (e.g., x-ray) radiation [33,34], particle acceleration [35,36], or the pumping of OPCPAs [37,38] have an avid demand for higher energies. Currently, however, the pulse energy obtained from such platforms has stagnated at the 200 mJ level.

Thin-disk based multipass amplifiers provide a simple and flexible platform to further increase pulse energies. By circumventing a closed optical resonator, and hence making an optical switch redundant, this platform enables unmatched pulse energies at high repetition rates. Multi-kilowatt output powers have been demonstrated with CPA-free multipass amplifiers, applied for materials processing [39,40]. Pulse energies above 1 Joule have been attained in a CPA multipass scheme at a repetition rate of 100 Hz [41]. The combination of Joule-class pulse energies with kW-class average powers has recently been demonstrated with a multipass amplifier using cryogenically cooled laser crystals. Here, pulse energies up to 1.5 J were extracted at 500 to 1000 Hz [42]. However, due to the strongly narrowed emission cross section at cryogenic temperatures, pulse durations of such cryogenic systems are typically limited to durations of ~4 ps [43].

Here, we present a Joule-class ultrafast thin-disk based multipass amplifier, developed as a transportable laser source for experimental campaigns within the framework of the LLR project. The 1-kHz CPA system produces up to 720-mJ pulses with a sub-picosecond pulse duration. The amplifier is operating at room temperature and under atmospheric pressure, simplifying the setup and auxiliary equipment. This allows for low maintenance operation at remote sites such as the Säntis station in Switzerland. The Joule-class pulse energy combined with an average power approaching the kilowatt range are unprecedented for such sub-picosecond laser systems operated at room-temperature. With these parameters, the laser system will be able to generate continuous, extended conductive channels, intended to eventually trigger atmospheric lightning discharges. First experiments of horizontal filament generation performed in the laboratory are promising for future extensive studies on the laser-based lightning rod [44].

2. Experimental setup

2.1. Overview of the laser system

The layout of the high-energy CPA laser amplifier is shown in Fig. 1. The system includes two main amplifier stages, namely, a regenerative amplifier followed by a high-energy multipass amplifier, both of which are based on the TRUMPF thin-disk technology. The whole system operates at room temperature and under atmospheric pressure, without any need for vacuum pumps or liquid gas supply (as required for cryogenically cooled laser systems). The overall dimensions including the compressor are 8.20 m in length and 1.40 m in width. The whole laser system is divided into five modules which are mounted onto a rigid aluminum frame structure. Castor wheels are attached to the frames, enabling mobility and transportability of the laser system. Centering pins allow for a precisely aligned reassembly of the laser modules at experimental sites after transport.

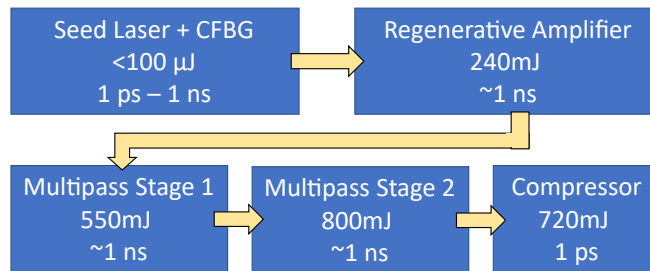


Fig. 1. Schematic flow-chart of the complete laser system. The seed pulses are stretched using a CFBG and amplified to 240 mJ in the regenerative amplifier. Further amplification takes place in the multipass stage 1 to 550 mJ and in the multipass stage 2 to 800 mJ. After compression, a pulse energy of 720 mJ and a pulse duration of <math><1</math> ps are obtained.

2.2. Seed laser

The seed laser is a commercial ultrafast laser typically used for micromachining (TruMicro 2000). It delivers typically femtosecond pulses centered around 1030 nm with an energy up to 100 μJ at a pulse-picked repetition rate of 1 kHz. The seed laser is fiber based and exhibits an excellent beam quality of typically $M^2 = 1.15$ [45]. For our purposes, the laser is equipped with a chirped fiber Bragg grating (CFBG) that temporally stretches the pulses to a duration of ~ 1 ns while the pulse compressor was removed for the following amplification.

2.3. Regenerative amplifier

The regenerative amplifier is based on the Dira 200-1 series, first presented by TRUMPF Scientific Lasers GmbH & Co. KG in 2015 [28]. It includes an industrial thin-disk laser head that is pumped by 940-nm laser diodes with up to 1 kW average pump power. A BBO-based Pockels cell combined with a thin-film polarizer (TFP) are used to couple in and out the pulses. The resonator of the regenerative amplifier is arranged in a ring configuration and designed for fundamental-mode operation. Within multiple resonator roundtrips, the pulse energy is amplified up to 240 mJ, while maintaining a near-diffraction limited beam quality with $M^2 < 1.2$. A monolithic, ruggedized housing provides excellent long-term stability, which is further improved by an active intracavity beam pointing stabilization, compensating for thermal drifts and reducing the warmup time to a few minutes. The output energy is actively stabilized via the pump power using feedback from an internal photodiode, allowing for a long-term stable operation. The shot to shot pulse energy stability is $<0.25\%$ (rms). The laser is fully automated by a ramp-up and alignment sequence, providing a turn-key high-energy ultrafast amplifier system.

2.4. Multipass amplifier

The multipass amplifier comprises four industrial thin-disk laser heads. Each laser head can be pumped with up to 10 kW of pump power at a wavelength of 940 nm. To minimize the thermal load on the disks, the disks are pumped in a quasi-continuous-wave regime with a duty cycle of 25% at the pulse repetition rate of 1 kHz. The heat load in the thin-disks causes a slight change of their refractive powers, inducing an additional small thermal lens. Several concepts have been investigated to ensure a stable propagation of the laser beam along the multipass amplifiers despite a variation of the thermal lens when operating at different pump powers. In 4- f -configurations, the plane of the thin-disk is continuously relay-imaged for each pass. This is advantageous to maintain a stable mode diameter on the thin-disk [46]. However, for intense laser pulses, the resulting foci in between the disk passes require operation in vacuum to prevent optical breakdown due to air ionization. Stable propagation can also be achieved with a concatenation of

resonator-like segments, however, at the cost of either small beam diameters at certain points along the propagation, or very long propagation distances [47,48]. Other approaches allow near-collimated propagation by balancing the beam divergence with a periodic focusing, which is provided by a well-chosen dioptric power of the thin-disk itself [39,49].

For our high-energy multipass amplifier, we designed a near-collimated propagation by means of refractive optics optimized for the thermal lens at the operation point. Due to the small divergence of the near-fundamental mode and large-diameter seed beam, the propagation is therefore stable only for small variations of the thermal lens. The amplifier requires accordingly a narrow pump power interval, which is experimentally determined to optimally balance the performance with respect to gain and beam quality. This approach allows to guide the seed beam over the thin-disks multiple times, each time with adjustable beam diameter using appropriate mirrors, depending on the evolved beam size and divergence. The complete multipass amplifier is arranged in two stages, as highlighted in Fig. 2(c). In the first stage, the pulses are amplified from 240 mJ to 550 mJ using 7 passes distributed on the two laser heads. In the second stage, the pulse energy is increased to 800 mJ via four additional disk reflections distributed on the laser heads 3 and 4. Curved mirrors can be placed conveniently between the two disks of each stage, eliminating transfer mirrors and reducing the overall propagation distance. Each disk is pumped with an average power of 2.3 kW. The super-Gaussian shaped pump spot has a diameter of approximately 12 mm. The cumulated total average pump power is >9 kW for the four amplifier heads, which is efficiently absorbed in the water-cooled disks, even without optical energy extraction. Stray pump light and fluorescence from the disk are mainly blocked by the pump head. The remaining portion of light exiting the pump head is dissipated by water-cooled structures, thereby strongly reducing thermal drifts of the mirror assembly in front of the disks. To further reduce and compensate for the residual thermal drift during operation, piezo-controlled mirrors are used to actively stabilize the beam pointing inside the multipass amplifier. Concepts to overcome thermal effects such as non-absorbing monolithic all-glass reflection arrays [39] were disregarded in this laser system but may be implemented for future systems.

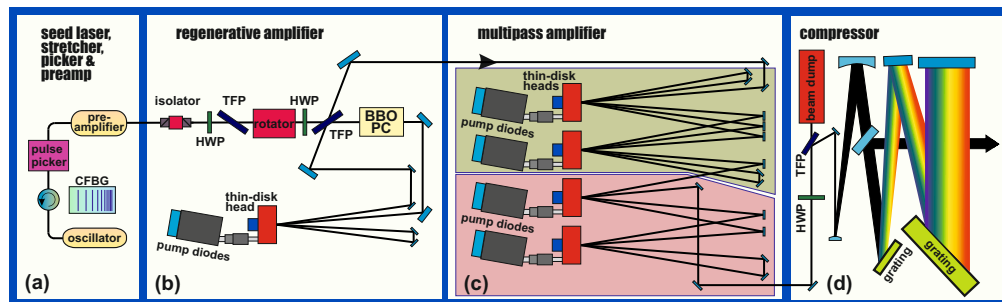


Fig. 2. Detailed sketch of the complete laser system. The seed pulses from the oscillator are stretched with a CFBG and first amplified by the regenerative amplifier, employing an industrial thin-disk laser head. The multipass contains 2 amplification stages, as indicated by the green (stage 1) and red (stage 2) areas. In each stage two industrial thin disk laser heads are employed. The grating compressor is set up in a folded Treacy-type near-Littrow configuration. TFP: Thin-film polarizer. HWP: Half-wave plate. BBO PC: BBO-based Pockels cell.

2.5. Grating compressor

The output pulses are compressed by a pair of multilayer dielectric (MLD) reflection gratings, arranged in a Treacy-type configuration under a near-Littrow angle of incidence [50]. The mechanical mounts for the large-size optics enable fine adjustment for tip, tilt, and in-plane

rotation [51] of the gratings for optimal alignment of the compressor. A total bandwidth of 5.0 nm is supported by the compressor configuration. The diffraction efficiency of each of the gratings is about 97%, leading to an overall compressor efficiency of $\sim 90\%$. At the full output power of the multipass amplifier (800 W uncompressed), 720 W average power were measured after compression, corresponding to a pulse energy of 720 mJ.

3. Results at high-power operation

In Fig. 3, the amplification slopes for the two stages of the multipass amplifier at high-energy operation are shown. The pump power is maintained constant while ramping up the seed pulse energy to 240 mJ, resulting in an amplified pulse energy of 550 mJ after stage 1 and 800 mJ after stage 2. From the measured curves, the tangential gain $G(E_{seed})$ at different seed pulse energies E_{seed} can be calculated according to

$$G(E_{seed}) = \frac{\Delta E_{out}}{\Delta E_{seed}}, \quad (1)$$

with E_{out} being the output pulse energy, which is shown with the dashed lines in Fig. 3. Here, the energy increments $\Delta E = E^n - E^{n-1}$ are calculated from two consecutive data points n and $(n-1)$. The tangential gain therefore defines the gain that an additional incremental multipass input pulse energy would experience. Hence, $G = 1$ implies a complete energy depletion, i.e. no further gain is to be expected despite an increase of seed energy.

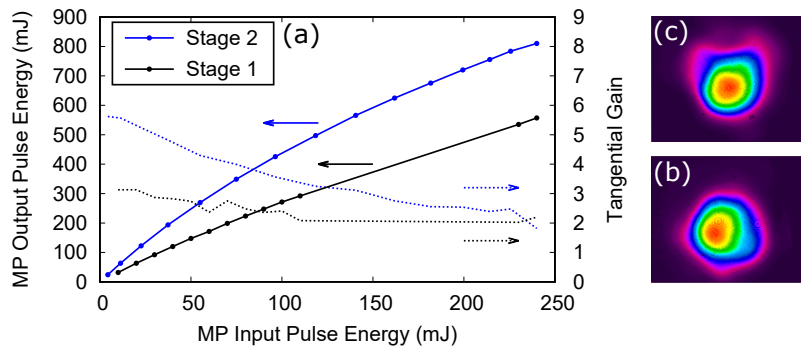


Fig. 3. Amplification characteristics of the multipass amplifier. (a) Output pulse energy of the two stages as a function of the seed pulse energy (solid lines, left-hand y-axis). The pump power is maintained at the operation point while ramping up the energy. The tangential gain is included as derived from the measurement (dashed lines, right-hand y-axis). (b) Beam profile of the collimated output after stage 1. (c) Beam profile of the collimated output after stage 2.

In consequence for the presented laser amplifier, it is important to note that it still has potential to generate pulse energies significantly higher than demonstrated in this paper. This can be inferred from the tangential gain at full seed energy $G(240 \text{ mJ})$ approaching a value of >2.3 . As a result, both stages are still operated in a regime far from reaching the saturation fluence, i.e. a significant amount of stored energy is still available in the laser disks. At the demonstrated point of operation with an output pulse energy of 800 mJ, an increase in seed pulse energy will still be amplified with a gain of >2.3 . The multipass could hence allow for even higher energies, enabled by a higher-energy seed source or further carefully implemented amplification passes while maintaining a good beam quality.

Typical near-field beam profiles of the collimated output beams of stages 1 and 2 can be seen in Fig. 3(b) and 3(c). Measurements to characterize the M^2 beam quality parameter of the

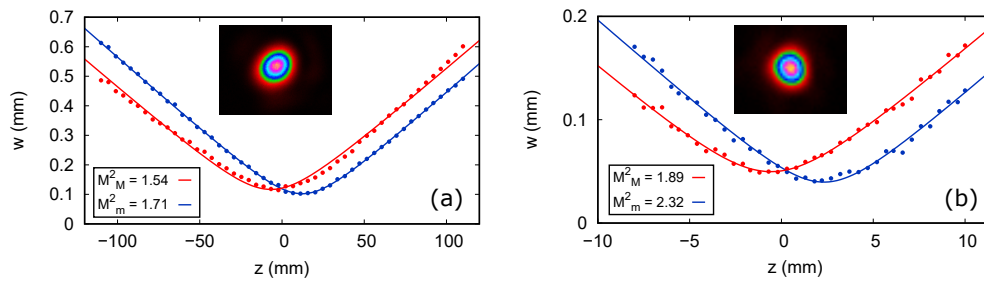


Fig. 4. Beam quality measurements of the high-power output. The insets contain the far-field beam profiles (a) Output beam of the multipass before compression. (b) Output beam after compression.

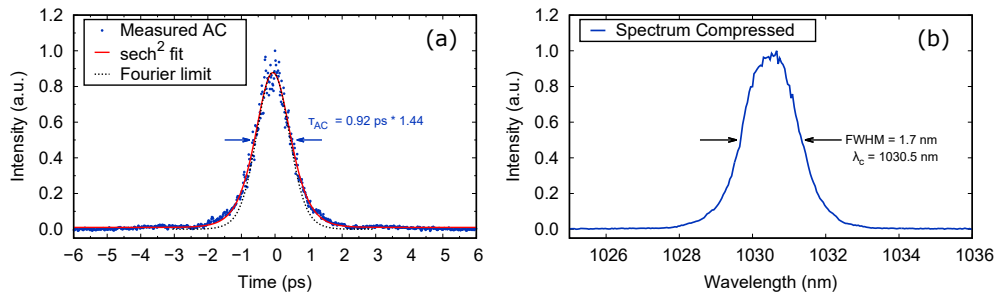


Fig. 5. Autocorrelation (AC) measurement and spectrum of the output pulses. (a) AC trace measured at full output power. The FWHM of the trace τ_{AC} is estimated from a sech^2 fit, resulting in a pulse duration of $\tau_{pulse} = 920$ fs. (b) Measured spectrum of the compressed output pulses. A spectral FWHM bandwidth of 1.7 nm is obtained at a center wavelength $\lambda_c = 1030.5$ nm.

uncompressed and compressed pulses were performed according to the ISO standard 11146, using a home-built linear stage in combination with a CCD camera, and applying the second moment method to determine the beam diameter in the major and minor axis [52]. Figure 4 shows the results of the M^2 measurements. For each measurement, the corresponding far-field beam profiles are presented as an inset. Before the compressor, we evaluated the average M^2 parameter to be 1.6 (1.54/1.71 for the major/minor axis) at a pulse energy of 800 mJ. After compression, i.e. at 720 mJ, this value increases to 2.1 (1.89/2.32 for the major/minor axis). The far-field beam profiles resemble smooth near-Gaussian modes in both cases. We attribute the

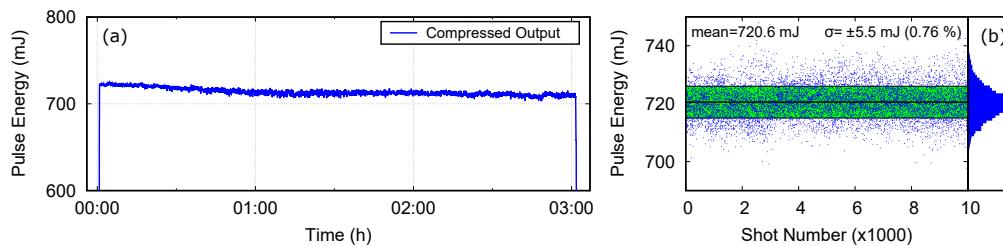


Fig. 6. Long-Term measurement of the output of the multipass amplifier after compression. (a) Diagram of the output pulse energy over time, measured with a calibrated photodiode. (b) Fast-time measurement of the pulse energy stability using 10,000 consecutive laser pulses measured by a calibrated photodiode.

degradation of the beam quality after compression primarily to the imperfect surface quality of the large-sized optics, as it was observed also at low compressed output power.

The pulse duration of the high-power compressor output was measured with an SHG autocorrelator. The measurement resulting in a pulse duration of $\tau_{pulse} = 920$ fs is plotted in Fig. 5(a). To obtain the deconvolution factor (1.44), the Fourier transform limited pulse shape as well as its autocorrelation function were calculated from the pulse spectrum. The peak power resulting from the measured pulse duration and pulse energy $E_{out} = 720$ mJ can be estimated via $P_{peak} = 0.88 \cdot E_{out} / \tau_{pulse} = 689$ GW, assuming a sech²-pulse shape. The spectrum was measured using a commercial grating spectrometer and is shown in Fig. 5(b). The corresponding spectral bandwidth is 1.7 nm (FWHM), which is mainly limited by gain narrowing during the overall amplification of the low-energy seed oscillator pulses by 45 dB. The generation of even shorter pulses, without significant modifications of the presented laser system, would be possible by pre-shaping the seed pulses spectrally, thus counteracting gain narrowing [53].

The long-term stability of the multipass amplifier was recorded over a time period of 3 hours, as shown in Fig. 6. The output energy was measured using a calibrated photodiode. The shot-to-shot pulse energy stability was measured over 10,000 consecutive shots [Fig. 6(b)], exhibiting a pulse-to-pulse energy stability of 0.76% (rms) and a near-Gaussian distribution.

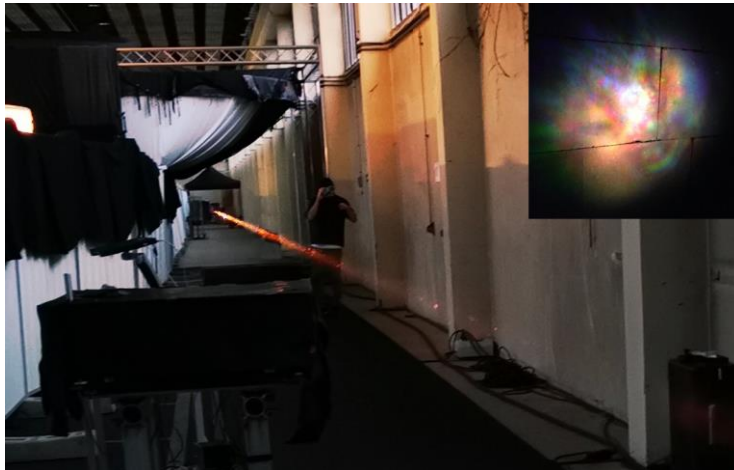


Fig. 7. White light from the filamentation of the collimated, compressed output beam at 720 mJ pulse energy. The emission scattered in forward direction is captured by the camera. The filament length was estimated to exceed 70 m, indicated by the darkening of photographic paper. The inset shows the white-light generated by the filament, visualized on the target (beam dump).

4. Generation of laser filaments

To test the generation of long-range filaments, the laser was installed inside the hall of an old linear accelerator (Laboratoire de l'Accélérateur Linéaire (LAL), Université Paris-Sud, France), providing up to ~ 200 m of straight distance for beam propagation. In a first experiment, the collimated output beam was directed to a beam dump at a distance of 130 m. By the darkening of photographic paper, filamentary structures could be detected over a range of >70 m. The scattered light from the laser beam in forward direction is visible in the photograph in Fig. 7. White light generated during the filamentation is emitted in the typical cone shape and could be observed on the concrete wall serving as a beam dump, as shown in the inset of Fig. 7. The

results are promising for future experiments planned in preparation for the field campaign of the LLR project. By employing a sending telescope, longer and remotely generated filaments will be enabled, ultimately used for the control of atmospheric lightning.

5. Summary and outlook

In summary, we have developed a Joule-class and kilowatt-level thin disk based sub-picosecond multipass amplifier system operating at room temperature and atmospheric pressure. The CPA laser system was developed for the Laser Lightning Rod project, aiming at the laser-based control and triggering of atmospheric lightning events via remote and long-range laser filamentation [18]. The system is currently providing long-term stable 720 mJ of pulse energy at a pulse duration of 920 fs at 1 kHz repetition rate, leading to a peak power of 689 GW. A beam quality of $M^2 = 2.1$ was measured at full output power. Further scaling of the pulse energy could be obtained by a higher energy extraction efficiency, via an increased seed energy or by adding more disk passes. Additionally, shorter pulse durations should be feasible by spectrally pre-shaping the seed oscillator pulses to pre-compensate for gain narrowing during amplification. Compensation of residual astigmatism would improve the output beam quality. With the developed laser source, first experiments were conducted to generate long-range filaments. A filament with a length exceeding 70 m could be achieved. Further experiments within the Laser Lightning Rod project will aim at increasing the filament length and the filamentation distance using a magnifying telescope.

Funding

Horizon 2020 Framework Programme (737033-LLR).

Acknowledgments

We gratefully acknowledge technical support from Marco Hartung, Yves-Bernard André, and Benoît Mahieu.

Disclosures

The authors declare no conflicts of interest.

References

1. A. Braun, G. Korn, X. Liu, D. Du, J. Squier, and G. Mourou, "Self-channeling of high-peak-power femtosecond laser pulses in air," *Opt. Lett.* **20**(1), 73–75 (1995).
2. P. Rohwetter, J. Kasparian, K. Stelmaszczyk, Z. Hao, S. Henin, N. Lascoux, W. M. Nakaema, Y. Petit, M. Queißer, R. Salamé, E. Salmon, L. Wöste, and J.-P. Wolf, "Laser-induced water condensation in air," *Nat. Photonics* **4**(7), 451–456 (2010).
3. Y. Liu, H. Sun, J. Liu, H. Liang, J. Ju, T. Wang, Y. Tian, C. Wang, Y. Liu, S. L. Chin, and R. Li, "Laser-filamentation-induced water condensation and snow formation in a cloud chamber filled with different ambient gases," *Opt. Express* **24**(7), 7364–7373 (2016).
4. S. Henin, Y. Petit, P. Rohwetter, K. Stelmaszczyk, Z. Q. Hao, W. M. Nakaema, A. Vogel, T. Pohl, F. Schneider, J. Kasparian, K. Weber, L. Wöste, and J.-P. Wolf, "Field measurements suggest the mechanism of laser-assisted water condensation," *Nat. Commun.* **2**(1), 456 (2011).
5. J. Kasparian, M. Rodriguez, G. Méjean, J. Yu, E. Salmon, H. Wille, R. Bourayou, S. Frey, Y.-B. André, A. Mysyrowicz, R. Sauerbrey, J.-P. Wolf, and L. Wöste, "White-Light Filaments for Atmospheric Analysis," *Science* **301**(5629), 61–64 (2003).
6. G. Méjean, J. Kasparian, J. Yu, S. Frey, E. Salmon, and J.-P. Wolf, "Remote detection and identification of biological aerosols using a femtosecond terawatt lidar system," *Appl. Phys. B* **78**(5), 535–537 (2004).
7. Q. Luo, H. L. Xu, S. A. Hosseini, J.-F. Daigle, F. Théberge, M. Sharifi, and S. L. Chin, "Remote sensing of pollutants using femtosecond laser pulse fluorescence spectroscopy," *Appl. Phys. B* **82**(1), 105–109 (2006).
8. G. Schimmel, T. Produit, D. Mongin, J. Kasparian, and J.-P. Wolf, "Free space laser telecommunication through fog," *Optica* **5**(10), 1338 (2018).

9. A. Hening, D. Wayne, M. Lovern, and M. Lasher, "Applications of laser-induced filaments for optical communication links," *Proc. SPIE* **9224**, 92240J (2009).
10. L. de La Cruz, E. Schubert, D. Mongin, S. Klingebiel, M. Schultze, T. Metzger, K. Michel, J. Kasparian, and J.-P. Wolf, "High repetition rate ultrashort laser cuts a path through fog," *Appl. Phys. Lett.* **109**(25), 251105 (2016).
11. J.-P. Wolf, "Short-pulse lasers for weather control," *Rep. Prog. Phys.* **81**(2), 026001 (2018).
12. B. Forestier, A. Houard, I. Revel, M. Durand, Y. B. André, B. Prade, A. Jarnac, J. Carbonnel, M. Le Nevé, J. C. de Miscault, B. Esmler, D. Chapuis, and A. Mysyrowicz, "Triggering, guiding and deviation of long air spark discharges with femtosecond laser filament," *AIP Adv.* **2**(1), 012151 (2012).
13. J. Kasparian and J.-P. Wolf, "Physics and Applications of atmospheric nonlinear optics and filamentation," *Opt. Express* **16**(1), 466–493 (2008).
14. X. M. Zhao, J. Diels, C. Y. Wang, and J. M. Elizondo, "Femtosecond ultraviolet laser pulse induced lightning discharges in gases," *IEEE J. Quantum Electron.* **31**(3), 599–612 (1995).
15. S. Uchida, Y. Shimada, H. Yasuda, S. Motokoshi, C. Yamanaka, T. Yamanaka, Z.-i. Kawasaki, and K. Tsubakimoto, "Laser-triggered lightning in field experiments," *J. Opt. Technol.* **66**(3), 199 (1999).
16. A. Couairon and A. Mysyrowicz, "Femtosecond filamentation in transparent media," *Phys. Rep.* **441**(2-4), 47–189 (2007).
17. T. Produit, G. Schimmel, E. Schubert, D. Mongin, A. Rastegari, C. Feng, B. Kamer, L. Arissian, J.-C. Diels, P. Walch, B. Mahieu, Y.-B. André, A. Houard, C. Herkommer, R. Jung, T. Metzger, K. Michel, A. Mysyrowicz, J.-P. Wolf, and J. Kasparian, "Multi-Wavelength Laser Control of High-Voltage Discharges. From the Laboratory to Sântis Mountain," in *Conference on Lasers and Electro-Optics*, OSA Technical Digest (Optical Society of America, 2019), paper JM2E.5.
18. "The Laser Lightning Rod project," (<http://lir-fet.eu>).
19. T. Produit, Groupe de Physique Appliquée, Université de Genève, Ch. de Pinchat 22, 1211 Genève 4, Switzerland, P. Walch, C. Herkommer, A. Mostajabi, M. Moret, U. Andral, A. Sunjerga, M. Azadifar, Y.-B. André, B. Mahieu, W. Haas, B. Esmler, G. Fournier, P. Krötz, T. Metzger, K. Michel, A. Mysyrowicz, M. Rubinstein, F. Rachidi, J. Kasparian, J. P. Wolf and A. Houard are preparing a manuscript to be called "The Laser Lightning Rod Project".
20. N. Jhaji, E. W. Rosenthal, R. Birnbaum, J. K. Wahlstrand, and H. M. Milchberg, "Demonstration of Long-Lived High-Power Optical Waveguides in Air," *Phys. Rev. X* **4**(1), 011027 (2014).
21. G. Point, E. Thouin, A. Mysyrowicz, and A. Houard, "Energy deposition from focused terawatt laser pulses in air undergoing multifilamentation," *Opt. Express* **24**(6), 6271–6282 (2016).
22. A. Houard, V. Jukna, G. Point, A.-B. André, S. Klingebiel, M. Schultze, K. Michel, T. Metzger, and A. Mysyrowicz, "Study of filamentation with a high-power high repetition rate ps laser at 1.03 μm ," *Opt. Express* **24**(7), 7437–7448 (2016).
23. P. Russbuehdt, T. Mans, J. Weitenberg, H. D. Hoffmann, and R. Poprawe, "Compact diode-pumped 1.1 kW Yb:YAG Innoslab femtosecond amplifier," *Opt. Lett.* **35**(24), 4169–4171 (2010).
24. P. Russbuehdt, G. Mans, J. Rotarius, J. Weitenberg, H. D. Hoffmann, and R. Poprawe, "400W Yb:YAG Innoslab fs-amplifier," *Opt. Express* **17**(15), 12230–12245 (2009).
25. M. Müller, A. Klenke, A. Steinkopf, H. Stark, A. Tünnermann, and J. Limpert, "3.5 kW coherently combined ultrafast fiber laser," *Opt. Lett.* **43**(24), 6037–6040 (2018).
26. H. Stark, J. Buldt, M. Müller, A. Klenke, A. Tünnermann, and J. Limpert, "23 mJ high-power fiber CPA system using electro-optically controlled divided-pulse amplification," *Opt. Lett.* **44**(22), 5529–5532 (2019).
27. C. J. Saraceno, D. Sutter, T. Metzger, and M. Abdou Ahmed, "The amazing progress of high-power ultrafast thin-disk lasers," *J. Eur. Opt. Soc.-Rapid Publ.* **15**(1), 15 (2019).
28. S. Klingebiel, M. Schultze, C. Y. Teisset, R. Bessing, M. Haefner, S. Prinz, M. Gorjan, D. H. Sutter, K. Michel, H. G. Barros, Z. Major, F. Krausz, and T. Metzger, "220mJ Ultrafast Thin-Disk Regenerative Amplifier," in *Conference on Lasers and Electro-Optics*, OSA Technical Digest (Optical Society of America, 2015), paper STu4O.2.
29. R. Jung, J. Tümmeler, and I. Will, "Regenerative thin-disk amplifier for 300 mJ pulse energy," *Opt. Express* **24**(2), 883–887 (2016).
30. T. Nubbemeyer, M. Kaumanns, M. Ueffing, M. Gorjan, A. Alismail, H. Fattahi, J. Brons, O. Pronin, H. G. Barros, Z. Major, T. Metzger, D. Sutter, and F. Krausz, "1 kW, 200 mJ picosecond thin-disk laser system," *Opt. Lett.* **42**(7), 1381–1384 (2017).
31. P. Krötz, C. Wandt, C. Grebing, C. Herkommer, R. Jung, S. Klingebiel, S. Prinz, C. Y. Teisset, K. Michel, and T. Metzger, "Towards 2 kW, 20 kHz ultrafast thin-disk based regenerative amplifiers," in *Laser Congress 2019 (ASSL, LAC, LS&C)*, OSA Technical Digest (Optical Society of America, 2019), paper ATh1A.8.
32. C. Wandt, C. Herkommer, R. Jung, S. Klingebiel, P. Kroetz, M. Rampp, C. Y. Teisset, K. Michel, and T. Metzger, "Ultrafast, Thin-Disk based CPA System with >1 kW Output Power and < 500 fs Pulse Duration," submitted to *Ultrafast Phenomena* (2020).
33. W. S. Graves, J. Bessuille, P. Brown, S. Carbajo, V. Dolgashev, K.-H. Hong, E. Ihloff, B. Khaykovich, H. Lin, K. Murari, E. A. Nanni, G. Resta, S. Tantawi, L. E. Zapata, F. X. Kärtner, and D. E. Moncton, "Compact x-ray source based on burst-mode inverse Compton scattering at 100 kHz," *Phys. Rev. Spec. Top.-Accel. Beams* **17**(12), 120701 (2014).

34. S. Wang, C. M. Baumgarten, Y. Wang, B. A. Reagan, A. P. Rockwood, H. Wang, L. Yin, K. Wernsing, H. Bravo, B. M. Luther, C. S. Menoni, and J. J. Rocca, "High-Power Ultrashort Pulse Lasers to Pump Plasma-Based Soft X-Ray Lasers," *IEEE J. Sel. Top. Quantum Electron.* **25**(4), 1–15 (2019).
35. F. Salehi, A. J. Goers, G. A. Hine, L. Feder, D. Kuk, B. Miao, D. Woodbury, K. Y. Kim, and H. M. Milchberg, "MeV electron acceleration at 1 kHz with <10 mJ laser pulses," *Opt. Lett.* **42**(2), 215–218 (2017).
36. A. J. Goers, G. A. Hine, L. Feder, B. Miao, F. Salehi, J. K. Wahlstrand, and H. M. Milchberg, "Multi-MeV Electron Acceleration by Subterawatt Laser Pulses," *Phys. Rev. Lett.* **115**(19), 194802 (2015).
37. S. Prinz, M. Haefner, C. Y. Teisset, R. Bessing, K. Michel, Y. Lee, X. T. Geng, S. Kim, D. E. Kim, T. Metzger, and M. Schultze, "CEP-stable, sub-6 fs, 300-kHz OPCPA system with more than 15 W of average power," *Opt. Express* **23**(2), 1388–1394 (2015).
38. T. Feng, A. Heilmann, M. Bock, L. Ehrentraut, T. Witting, H. Yu, H. Stiel, S. Eisebitt, and M. Schnürer, "27 W 2.1 μ m OPCPA system for coherent soft X-ray generation operating at 10 kHz," *Opt. Express* **28**(6), 8724–8733 (2020).
39. T. Dietz, M. Jenne, D. Bauer, M. Scharun, D. Sutter, and A. Killi, "Ultrafast thin-disk multi-pass amplifier system providing 19 kW of average output power and pulse energies in the 10 mJ range at 1 ps of pulse duration for glass-cleaving applications," *Opt. Express* **28**(8), 11415–11423 (2020).
40. J.-P. Negel, A. Loescher, D. Bauer, D. Sutter, A. Killi, M. A. Ahmed, and T. Graf, "Second Generation Thin-Disk Multipass Amplifier Delivering Picosecond Pulses with 2 kW of Average Output Power," in *Laser Congress 2016 (ASSL, LSC, LAC)*, OSA Technical Digest (Optical Society of America, 2016), paper ATu4A.5.
41. R. Jung, J. Tümmler, T. Nubbemeyer, and I. Will, "Two-Channel Thin-Disk Laser for High Pulse Energy," in *Advanced Solid State Lasers*, OSA Technical Digest (Optical Society of America, 2015), paper AW3A.7.
42. B. A. Reagan, C. Baumgarten, E. Jankowska, H. Chi, H. Bravo, K. Dehne, M. Pedicone, L. Yin, H. Wang, C. S. Menoni, and J. J. Rocca, "Scaling diode-pumped, high energy picosecond lasers to kilowatt average powers," *High Power Laser Sci. Eng.* **6**, e11 (2018).
43. J. Dong, M. Bass, Y. Mao, P. Deng, and F. Gan, "Dependence of the Yb³⁺ emission cross section and lifetime on temperature and concentration in yttrium aluminum garnet," *J. Opt. Soc. Am. B* **20**(9), 1975–1979 (2003).
44. T. Produit, P. Walch, G. Schimmel, B. Mahieu, C. Herkommer, R. Jung, T. Metzger, K. Michel, Y.-B. André, A. Mysyrowicz, A. Houard, J. Kasparian, and J.-P. Wolf, "HV discharges triggered by dual- and triple-frequency laser filaments," *Opt. Express* **27**(8), 11339–11347 (2019).
45. TRUMPF Laser GmbH, "Data Sheet TruMicro Series 2000," https://www.trumpf.com/no_cache/de_DE/produkte/laser/kurz-und-ultrakurzpuls-laser/tru-micro-serie-2000/product_data_sheet/download/TRUMPF-technical-data-sheet-TruMicro-Serie-2000.pdf.
46. S. Keppler, C. Wandt, M. Hornung, R. Bödefeld, A. Kessler, A. Sävert, M. Hellwing, F. Schorch, J. Hein, and M. C. Kaluza, "Multipass amplifiers of POLARIS," *Proc. SPIE* **8780**, 878001 (2013).
47. K. Schuhmann, K. Kirch, M. Marszalek, F. Nez, R. Pohl, I. Schulthess, L. Sinkunaite, G. Wichmann, M. Zeyen, and A. Antognini, "Multipass amplifiers with self-compensation of the thermal lens," *Appl. Opt.* **57**(35), 10323 (2018).
48. K. Schuhmann, M. A. Ahmed, A. Antognini, T. Graf, T. W. Hänsch, K. Kirch, F. Kottmann, R. Pohl, D. Taqqu, A. Voss, and B. Weichelt, "Thin-disk laser multi-pass amplifier," *Proc. SPIE* **9342**, 93420U (2015).
49. J.-P. Negel, A. Loescher, B. Dannecker, P. Oldorf, S. Reichel, R. Peters, M. Abdou Ahmed, and T. Graf, "Thin-disk multipass amplifier for fs pulses delivering 400 W of average and 2.0 GW of peak power for linear polarization as well as 235 W and 1.2 GW for radial polarization," *Appl. Phys. B* **123**(5), 156 (2017).
50. E. Treacy, "Optical pulse compression with diffraction gratings," *IEEE J. Quantum Electron.* **5**(9), 454–458 (1969).
51. B. Webb, M. J. Guardalben, C. Dorrer, S. Bucht, and J. Bromage, "Simulation of grating compressor misalignment tolerances and mitigation strategies for chirped-pulse-amplification systems of varying bandwidths and beam sizes," *Appl. Opt.* **58**(2), 234–243 (2019).
52. J. Eichler, L. Dünkel, and B. Eppich, "Die Strahlqualität von Lasern – Wie bestimmt man Beugungsmaßzahl und Strahldurchmesser in der Praxis?" *Laser Tech. J.* **1**, 63–66 (2004).
53. S. Klingebiel, C. Wandt, M. Siebold, Z. Major, I. Ahmad, S. Trushin, R. Hörlein, T.-J. Wang, F. Krausz, and S. Karsch, "Counteracting gain narrowing using spectral amplitude shaping in a high-energy diode-pumped CPA system based on Yb-doped materials," in *Advanced Solid-State Photonics*, OSA Technical Digest (Optical Society of America, 2009), paper TuB9.